Biofabrication of bacterial nanocellulose scaffolds with complex vascular structure

Biofabrication

International Society for Biofabrication

Biofabrication of bacterial nanocellulose scaffolds with complex vascular structure

Biofabrication

PAPER

Biofabrication of bacterial nanocellulose scaffolds with complex vascular structure

Sanna Sämfors[1,5], Kristina Karlsson[2,5], Johan Sundberg[3,5], Kajsa Markstedt[3] and Paul Gatenholm[3,4]

[1] Department of Chemistry and Chemical Engineering, Analytical Chemistry, Chalmers University of Technology, Gothenburg, Sweden
[2] Department of Materials and Manufacturing Technology, Polymeric Materials and Composites, Chalmers University of Technology, Gothenburg, Sweden
[3] Department of Chemistry and Chemical Engineering, Biopolymer Technology, Wallenberg Wood Science Center, Chalmers University of Technology, Gothenburg, Sweden
[4] CELLHEAL AS, Sandvika, Norway
[5] These authors contributed equally to this work.

E-mail: paul.gatenholm@chalmers.se

Keywords: bacterial nanocellulose, tissue engineering, vascular mimetic, HUVECs, 3D printing

OPEN ACCESS

RECEIVED
19 November 2018

REVISED
31 May 2019

ACCEPTED FOR PUBLICATION
20 June 2019

PUBLISHED
25 July 2019

Abstract

Bacterial nanocellulose (BNC) has proven to be an effective hydrogel-like material for different tissue engineering applications due to its biocompatibility and good mechanical properties. However, as for all biomaterials, *in vitro* biosynthesis of large tissue constructs remains challenging due to insufficient oxygen and nutrient transport in engineered scaffold-cell matrices. In this study we designed, biofabricated and evaluated bacterial nanocellulose scaffolds with a complex vascular mimetic lumen structure. As a first step a method for creating straight channeled structures within a bacterial nanocellulose scaffold was developed and evaluated by culturing of Human Umbilical Vein Endothelial Cells (HUVECs). In a second step, more complex structures within the scaffolds were produced utilizing a 3D printer. A print mimicking a vascular tree acted as a sacrificial template to produce a network within the nanoporous bacterial nanocellulose scaffolds that could be lined with endothelial cells. In a last step, a method to produce large constructs with interconnected macro porosity and vascular like lumen structure was developed. In this process patient data from x-ray computed tomography scans was used to create a mold for casting a full-sized kidney construct. By showing that the 3D printing technology can be combined with BNC biosynthesis we hope to widen the opportunities of 3D printing, while also enabling the production of BNC scaffolds constructs with tailored vascular architectures and properties.

Introduction

In vitro biosynthesis of large tissue constructs remains challenging due to insufficient oxygen and nutrient transport in engineered scaffold-cell constructs. Smaller constructs can rely upon diffusion of media through the scaffold for mass transfer, but in larger constructs the diffusion is not sufficient since the critical length of oxygen diffusion is approximately 100–200 μm [1, 2]. Cells that are not located directly at or in close proximity to the scaffold surface do not receive an adequate supply of oxygen nor nutrients. Introducing porosity to scaffolds can be a way to increase nutrient transport [3]. For *in vivo* applications it has been seen that porous materials with a pore size larger than 250 μm have a faster in-growth of vessels than scaffolds with smaller pores facilitating oxygen transfer and subsequently host tissue integration [4, 5]. Numerous approaches have been explored to introduce vascular networks in scaffolds, from scaffold design [6–9] and co-cultures [10] to the use of vascular endothelial growth factors to enhance the angiogenesis [11, 12]. If the implant already contains vascular growth factors this could increase the speed of vascularization. However, if the implant is large it may still take days to weeks, depending on the size, for the interior of the implant to be completely vascularized [13] leading to cell death and subsequent implant/construct failure.

One approach to increase scaffold vascularization has been to introduce micro channels and oriented pores in different types of scaffolds to increase mass transfer and to aid guidance of cells [14–17]. It has also been shown that channeled scaffolds enhance cellular density in perfused scaffolds [18]. Micro channeled scaffolds have been used for meniscus growth [19] liver fabrication [20], cardiac tissue applications [21] and nerve regeneration [22, 23]. The developments of additive manufacturing techniques [24–29] has enabled the production of complex 3D structures with incorporated vascular structures [9, 30–32]. Scaffolds can be customized according to the data acquired from medical scans to match each patient's individual needs.

Hydrogels have shown great promise as scaffold material [33]. Bacterial nanocellulose (BNC) consist of an interconnected network of cellulose ribbons [34, 35] and has been proven to be an effective hydrogel-like material for different tissue engineering applications due to its biocompatibility and good mechanical properties for various tissue engineering constructs [36–39]. After washing with NaOH, BNC scaffolds have been shown to have endotoxin levels well below the threshold for medical devices and they are non-cytotoxic [40]. It has been shown to be blood compatible and has previously been used for tissue engineered blood vessels [41–43]. Controlled three dimensional shapes of BNC have been achieved by culturing bacteria in molds and by 3D printing bacteria [44–46]. The porosity of native BNC does not allow for cell penetration but BNC can be made porous by different techniques [47–50] and act as a scaffold for several different cell types [36, 38, 49, 51]. However, engineering small complex features mimicking native tissue within BNC still provides a challenge.

In this study we designed, biofabricated and evaluated BNC scaffolds with different vascular mimetic structure. First, a method for creating channeled structures within a nanoporous BNC scaffolds was developed and evaluated by culturing of Human Umbilical Vein Endothelial Cells (HUVECs) seeded on and within the scaffold channels. Secondly, more complex structures were created within nanoporous BNC scaffolds utilizing a 3D printer. A print mimicking a vascular tree acted as a sacrificial template to produce a network within the nanoporous BNC scaffolds. The channeled network within the scaffold was lined with HUVECs to mimic a vascular network. Finally, an attempt towards producing a large construct with interconnected macro porosity and a vascular like structure was made. In this process patient data from CT scans was used to create a mold for casting a full-sized kidney mimetic construct. In this work, we show that 3D printing technology can be combined with BNC biosynthesis to create scaffolds with tailored morphology and complex small features to be used for vascular mimetic applications.

Materials and methods

Clay-needle template production

Clay-needle templates were manufactured using a linear actuator (Singer) with a needle (0.25 × 15 mm) (Hegu). Holes were punched into clay (Panduro) with an inter-distance of 1 mm. The clay was allowed to cure at 110 °C. Needles were then inserted into the holes (figure 1(A)). The templates were autoclaved (Varioklav 135 T, (121 °C, 20 min)) prior to use.

Bacterial culture media

Bacterial culture media was prepared according to Matsuoka *et al* [52]. In short, the media was prepared by mixing fructose (40 g l^{-1}), yeast extract (5 g l^{-1}), $(NH_4)_2SO_4$ (3.3 g l^{-1}), KH_2PO_4 (1 g l^{-1}), $MgSO_4 \cdot 7H_2O$ (0.25 g l^{-1}), corn steep liquor (20 ml l^{-1}), trace metal solution (10 ml l^{-1}) and vitamin solution (5 ml l^{-1}). The solution was pH adjusted to 5.0 and filter sterilized.

Bacterial nanocellulose scaffold biosynthesis

Bacterial culture in bacterial culture media (*Gluconacetobacter Xylinus* (Acetobacter Xylinum susp. Sucrofermentas BPR2001, ATCC No. 700178)) was added to the templates to cover 2/3 of the needles. The cultures were incubated at 30 °C for 72 h. The BNC pellicles were removed from the needle templates and washed in NaOH (0.5 M). The NaOH was replaced twice a day for 3 d. The BNC was then washed in deionized (DI) water, which was replaced twice a day until the pH reached 7.0. The channeled parts were punched out using a biopsy punch (8 mm) and autoclaved (Varioklav 135 T, (121 °C, 20 min)) prior to *in vitro* cell culture.

3D printing of sacrificial PLA template

A MakerBot Replicator™2 (MakerBot) desktop 3D printer was used to produce vascular tree [53] mimetic sacrificial templates. The printer had a layer resolution height of 100 μm and a nozzle diameter of 400 μm. The nozzle was heated to 230 °C to melt extrude polylactic acid (PLA).

Incorporation of PLA sacrificial templates in BNC pellicles

BNC pellicles for incorporation of PLA sacrificial templates were produced in 95 ml Petri-dishes. All samples were incubated at 30 °C. PLA templates, sterilized in 70% ethanol for 20 min, were placed on top of the growing pellicles after 3 d. Care was taken when placing the PLA templates to avoid disturbance of the cultures to avoid pellicle layer separation. The cultures were incubated for another 3 d, until the PLA templates structures were completely incorporated in the pellicles. The BNC pellicles were washed in NaOH (0.5 M) for 10 d at 60 °C until the pellicles were completely translucent white. The NaOH was exchanged twice a

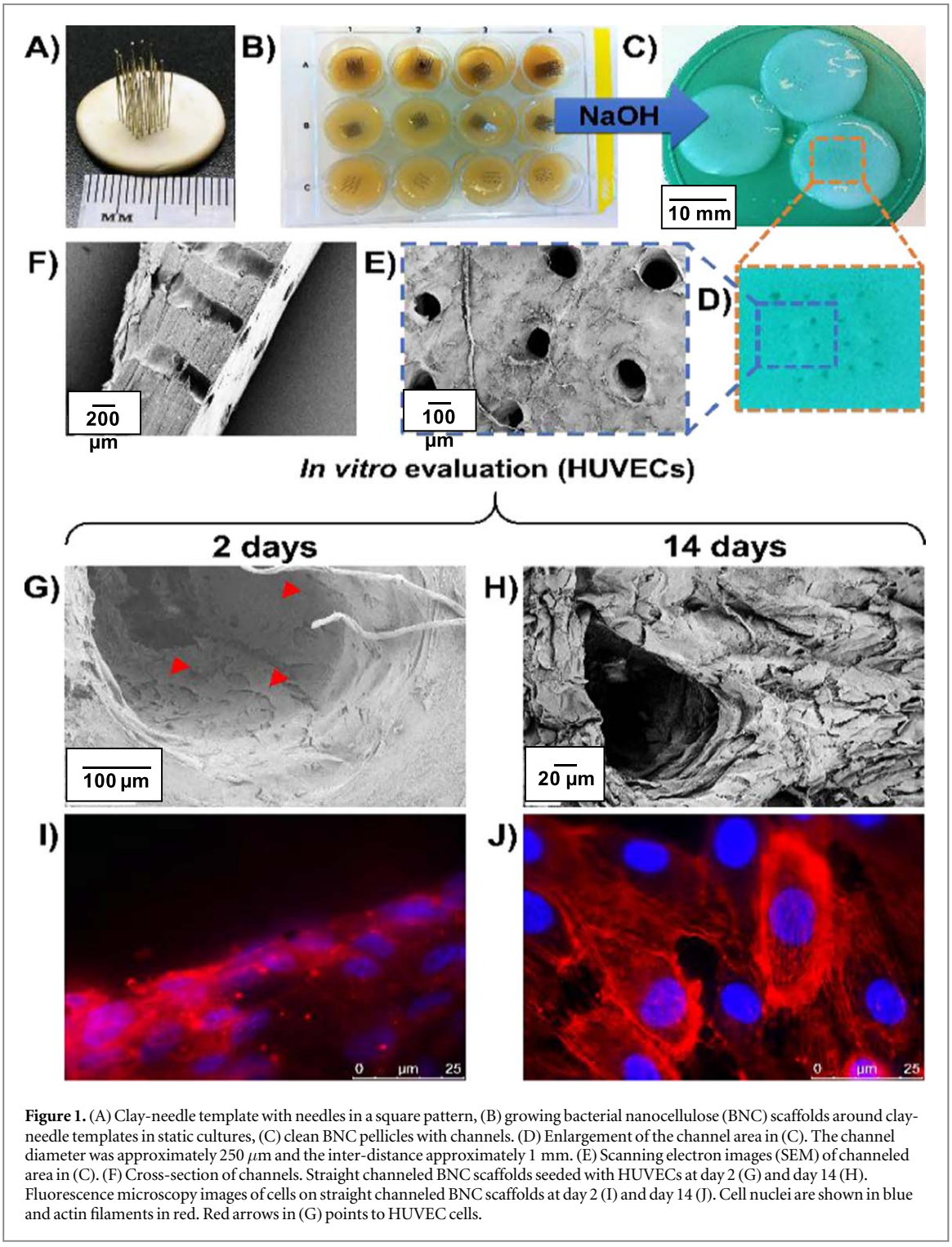

Figure 1. (A) Clay-needle template with needles in a square pattern, (B) growing bacterial nanocellulose (BNC) scaffolds around clay-needle templates in static cultures, (C) clean BNC pellicles with channels. (D) Enlargement of the channel area in (C). The channel diameter was approximately 250 μm and the inter-distance approximately 1 mm. (E) Scanning electron images (SEM) of channeled area in (C). (F) Cross-section of channels. Straight channeled BNC scaffolds seeded with HUVECs at day 2 (G) and day 14 (H). Fluorescence microscopy images of cells on straight channeled BNC scaffolds at day 2 (I) and day 14 (J). Cell nuclei are shown in blue and actin filaments in red. Red arrows in (G) points to HUVEC cells.

day. The pellicles were then transferred to a 90 °C shaking water bath for 24 h. In this process, the sacrificial PLA templates were hydrolyzed and leeched out of the BNC. The pellicles were washed in DI water until the pH reached 7.0. The DI water was exchanged twice a day. The pellicles were autoclaved (Varioklav 135 T, (121 °C, 20 min)) prior to *in vitro* cell culture.

Expansion of HUVECs

Endothelial basal media (Cell Applications, Inc.) was mixed with endothelial growth supplements (Cell Applications, Inc.) to create Endothelial Cell Growth Media (ECG media). A vial of human umbilical vein endothelial cells (HUVECs) (Cell Applications, Inc.) was thawed in a water bath at 37 °C. The cells were transferred to a 75 cm^2 cell culture flask containing 15 ml of ECG media; this was denoted passage 1. The cell culture flask was incubated (Forma Steri-Cycle 371, Thermo Scientific) (37 °C, 5% CO_2, 95% relative humidity). The cells were split when reaching 80% confluence. Cells at passage number 4 were used for all the cell experiments.

Seeding of HUVECs on straight channeled scaffolds

Before cell seeding, the straight channel scaffolds were incubated in ECG media for 1 h. The scaffolds were dried on filter paper for 1 s on each side to remove media in the channels, and placed in a 24-well plate, one scaffold in each well. 200 μl of cell suspension was seeded on the scaffolds at a cell density of 3×10^5 cell cm^{-2}. The total area was calculated as the sum of the surface area plus the lumen wall area. The well plate incubated (Forma Steri-Cycle 371, Thermo Scientific) (37 °C, 5% CO_2, 95% relative humidity) for 4 h to allow optimal cell attachment. 1.5 ml of ECG media was added to each scaffold and the well plate was placed back into the incubator, this was denoted as day 0. Media was changed every 2–3 d and samples were taken at day 2, day 4, day 7 and day 14.

Scanning electron microscopy (SEM)

Samples taken for SEM analysis were washed in PBS twice to get rid of media residues, then covered in 2.5% glutaraldehyde (Sigma-Aldrich) in PBS and left for 2 h at room temperature. Samples were rinsed twice in PBS and dehydrated in baths of increasing ethanol concentration (70%, 80%, 90%, 95% and 99%). The samples were placed in t-butanol, frozen at −80 °C and freeze dried in a lyophilizer (Heto, PowerDry, PL3000). Before analysis the samples were sputter coated (Sputter Coater s150B, Edwards) with gold. The SEM analysis was performed with a Leo Ultra 55 FEG-SEM.

Fluorescence microscopy

Samples for fluorescence microscopy analysis were washed in PBS twice to get rid of media residues, then covered in 3.7% formaldehyde (Sigma- Aldrich) in PBS and left for 2 h at room temperature. Samples were rinsed twice in PBS and transferred to 60% ethanol where they were kept until analysis. Before analysis the scaffolds were rinsed in PBS twice. 0.1% Triton X100 (Sigma-Aldrich) in PBS was added to cover the samples and left for 45 min. The solution was removed and the samples were washed twice in PBS. Rhodamine phalloidin in PBS (10 $\mu m\ ml^{-1}$) was added to cover the samples and left for 30 min. The solution was aspirated and DAPI in PBS (5 $\mu m\ ml^{-1}$) was added to cover the samples for 30 min. Rhodamine phalloidin was used to visualize the actin filaments and DAPI was used to stain cell nuclei. The samples were rinsed twice in PBS and stored in PBS until visualization. For analysis, a phase contrast microscope (Leica Digital Microscopes Inverted) was used together with the software Leica LAS AF.

Seeding of HUVECs on complex scaffolds

Before cell seeding, the BNC pellicles were incubated in ECG media for 1 h. HUVECs at the same concentration as for the straight channeled scaffolds were seeded by injection with a thin needle into the vascular like channel structure incorporated in the pellicles. The total lumen volume was approximately 40 μl given by the weight and density of the PLA templates. Care was taken to avoid introduction of air into the channel during the seeding and the injection was done at a slow pace to minimize potential shear stress damage of the cells. The pellicles were placed in a 6-well plate, one pellicle in each well. The well plate was incubated (Forma Steri-Cycle 371, Thermo Scientific) (37 °C, 5% CO_2, 95% relative humidity) for 4 h. After 2 h, the scaffolds were turned upside down to allow optimal cell attachment. 3 ml of ECG media was then added to each scaffold, this was denoted as day 0. Media was changed every 2–3 d and samples were taken at day 1, day 4 and day 7.

Confocal microscopy

At day 1, 4 and 7, complex scaffold samples were taken for confocal microscopy analysis. The same protocol as for fluorescent microscopy analysis was used to stain the samples for confocal microscopy analysis. Stained samples were placed under 0.17 mm cover glass slips and visualized using a LSM710MP instrument (Carl Zeiss) with a W Plan-Apochromat 20×/1.0 DIC D = 0.17 M27 75 mm objective and pinhole set to 31 μm for each channel.

Production of BNC/Alginate mixture

Porous BNC scaffolds were produced by homogenizing BNC with a blender until a pulp consistency was obtained, and then further blended with a dispersing element (S25N-18G,IKA, Germany) at 25 000 rpm for 20 min. The cellulose content of the homogenized BNC was measured using a Halogen Moisture Analyzer (HB43, Mettler Toledo). 1.1% w/w clinical grade alginate derived from brown algae dissolved in 0.9% NaCl (Cellmed AG) was added to the homogenized BNC to get a final composition of 90% dry weight BNC and 10% dry weight alginate compared to the total dry weight. After mixing of the BNC and alginate, the solution was blended using an IKA T25 homogenizer for 20 min until it reached a slurry-like consistency.

Production of macro porous scaffolds using clay-needle templates

Clay-needle templates were covered in the BNC/alginate mixture in 125 ml plastic containers. The mixture was degassed in a vacuum-chamber. After degassing the samples were placed in a Nalgene Cryo 1 °C min^{-1} freezing container (Mr Frosty) in a −80 °C freezer for 24 h. After 24 h, the samples were removed and gently heated until released from the container. The samples were returned to the −80 °C freezer for 2 h before they were freeze dried (Heto PowerDry PL3000) until completely dry.

Kidney mimetic scaffold production

The CT-data were kindly provided by Andreas Hultgren at Karolinska University Hospital. The data was anonymized and patients consent was given in accordance with the ethical guidelines. Slicer (32 bit version 4.2.2–1) was used to convert abdominal CT-scans into 3D surface models of kidneys. The contour of the kidneys was digitally optimized to increase the segmentation selectivity. Image segmentation was done using thresholding, which created a label map of the selected area. After segmentation, a surface model was created using the model maker module. The model was saved as a .STL file. The model did not include any internal features such as vasculature.

The .STL file was loaded to MakerWare (MakerBot) and 3D printed using a MakerBot Replicator™2 (MakerBot). The PLA kidney was used as a template to produce a negative mold with clay (Panduro). The clay mold was cured in an oven at 110 °C. Degassed BNC/alginate mixture was added to the clay mold. A sacrificial PLA template was inserted and the mold was then placed in a Nalgene Cryo 1 °C min^{-1} freezing container (Mr Frosty) in a −80 °C freezer for 24 h. After 24 h, the mold was removed and gently heated to allow for the frozen mixture to release from the mold. The frozen kidney shaped BNC/alginate mixture was returned to the −80 °C freezer for 2 h and then freeze dried (Heto PowerDry PL3000) until completely dry. The sponge was cross-linked by submersion in 100 mM $CaCl_2$ solution. The PLA sacrificial template was left in the freeze-dried structure and the kidney constructs were not evaluated by a cell study.

Results and discussion

Clay-needle templates (figure 1(A)) were used during the biosynthesis of BNC (figure 1(B)) to create straight channels in nanoporous BNC scaffolds (figures 1(C)–(F)). After 3 d of culture, pellicles of bacterial nanocellulose with a thickness of 3 mm had formed at the air-liquid interface (figure 1(B)). The structure of the channels was maintained after template removal and only slight collapse or occlusion of the channels were seen. The small collapse of some of the channels (e.g. figure 1(H)) is believed to be due to the sample preparation before SEM analysis where the scaffolds is dried. The drying process will cause the hydrogel to slightly disform. The dimensions of the channels were limited by the needle diameter (250 μm) and in figure 1(F) the channels can be seen intact throughout the length of the scaffold. The lumen wall of the channels had low porosity and only mild texturing probably facilitating endothelial cell attachment (figures 1(G)–(J)). Figures 1(G)–(H) shows SEM images of the straight channeled scaffolds seeded with HUVECs. Cells were found on all the samples (red arrows in figure 1(G)) and were located on top of the scaffolds and inside the channels. During the *in vitro* evaluation, the cells proliferated and gained a more outstretched morphology indicating good cellular adhesion to the scaffold. Figures 1(I)–(J) shows fluorescence microscopy images of cells on channeled scaffolds. The cells were stained with DAPI to visualize cell nuclei (shown in blue) and rhodamine phalloidin to visualize the actin filaments (shown in red). At day 14 a monolayer of cells could be seen on the scaffolds (figure 1(J)).

In order to fabricate scaffolds with higher complexity of the internal lumen structure sacrificial PLA templates were produced by a MakerBot Replicator 2X (MakerBot) (figures 2(A)–(B)). A flat tree like structure with several closed loops was chosen to simulate a vascular system. The dimensions of the template features were limited by the printer head nozzle, where the diameter of the nozzle was 400 μm and the layer resolution height was 100 μm. Future improvements to the hardware will likely enable production of templates with smaller features resembling the dimensions of capillaries. The bacteria synthesize nanocellulose at a rate of approximately 1 mm in thickness per 24 h. The cellulose production occurs at the air/growth medium interface and objects placed on the top of the growing pellicle can be incorporated into the hydrogel nanocellulose pellicle. The PLA sacrificial templates were successfully incorporated into BNC pellicles (figure 2(C)) and then removed by hydrolysis of the PLA during the NaOH purification process of the BNC (figure 2(D)), leaving a complex vascular like channel system within the nanoporous BNC scaffolds. In figures 2(E)–(F) the lumen structure within a BNC pellicle, after PLA template removal, is visualized by injection of a hydrophobic dye (Blue dye tracer (Bahrdahl Industry)). As seen the template removal was complete and the integrity of the channels was intact.

The complex channeled nanoporous BNC scaffolds were seeded with HUVECs. The cells were stained with DAPI and rhodamine phalloidin and the cells were visualized under a confocal microscope at day 1, 4 and 7 as seen in figures 2(G)–(H). At day 1 the cells were found throughout the scaffold channels and the cells had a round morphology. Until day 4 the cells stretched and covered the lumen of the scaffold channels. No specific cell orientation was apparent. At day 7 there were some indication of cells starting to align in a unidirectional manner. The result of the evaluation of the straight channeled scaffolds and the complex scaffolds showed that it is possible to create ordered channeled systems within nanoporous BNC using clay-needle constructs and 3D printed sacrificial templates. These scaffolds could then be cellularized with HUVECs, which after approximately 7 d started to form a monolayer of cells on lumen wall of the channels. In the cell studies performed on the straight channeled and the complex channeled scaffolds cells could be found on all the scaffolds at all time points. Due to the lack of macro-porosity in between the channels we believe that these types of scaffolds could

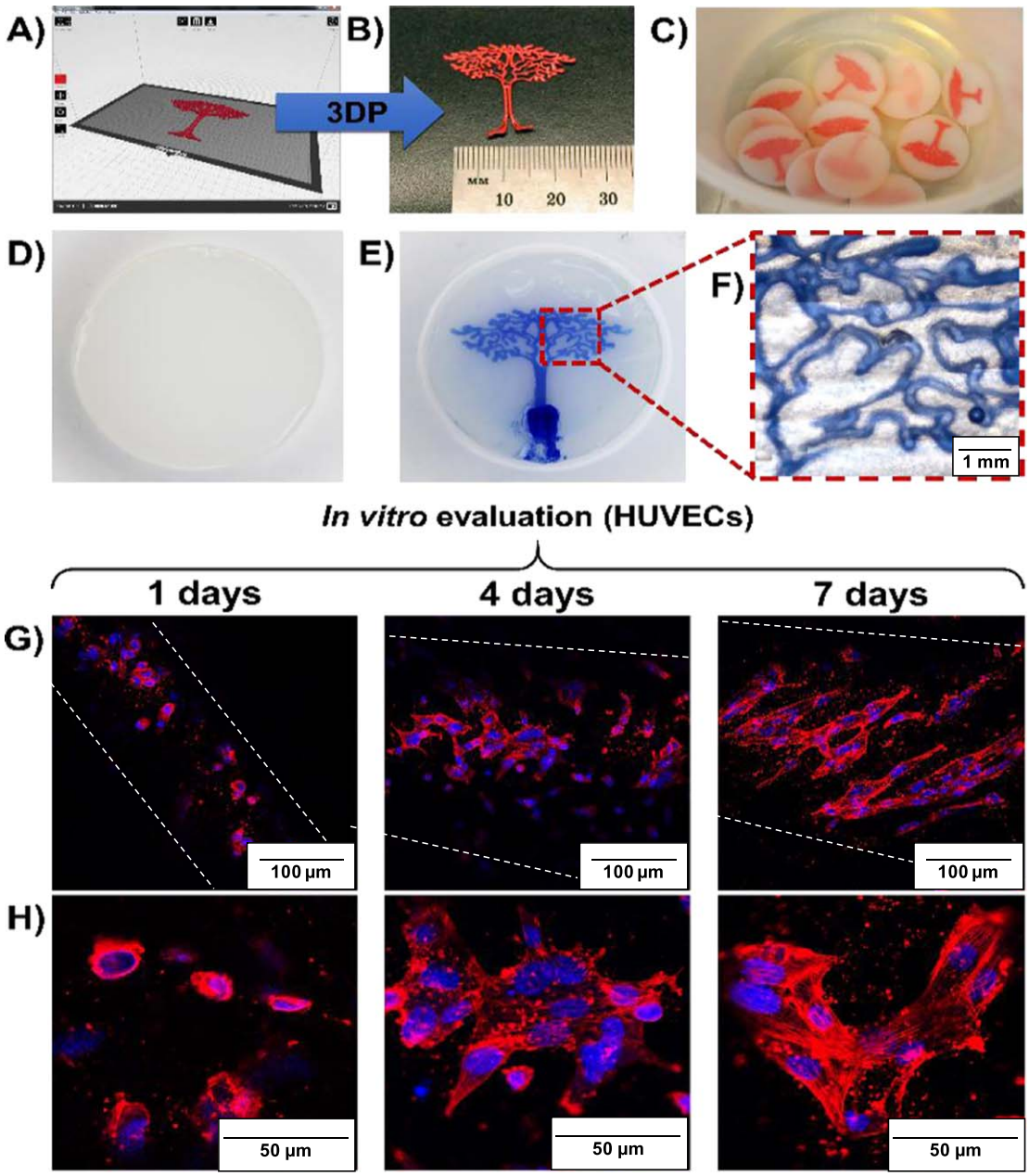

Figure 2. (A) Stereo lithography file (.STL) of complex tree model simulating a vascular system displayed in software MakerWare. (B) 3D printed poly lactic acid (PLA) sacrificial template. (C) PLA sacrificial templates incorporated in BNC pellicles. (D) BNC pellicle after cleaning after template removal. No traces of the template or any lumen structure visible. (E) A blue dye tracer injected into the lumen structure in order to visualize the channels. (F) Inverted light microscopy landscape image at 4× magnification of the pellicle injected with the hydrophobic dye. As seen the template removal seems complete and the integrity of the channels seems intact. (G) and (H) Confocal microscopy images at two different magnifications of BNC scaffolds with complex vascular structure seeded with HUVECs at day 1, day 4 and day 7. Cell nuclei are shown in blue and actin filaments in red. White dashed lines show proposed outline of channel.

be used to model vascular systems or other tubular tissues with tailored morphology *in vitro*.

In order to make a successful tissue mimetic construct, the space in between the vascular lumens needs to be macro-porous to allow for additional cells to be incorporated and to interact with the vascular system. By freeze casting homogenized BNC blended with alginate (figure 3(A)) porous scaffolds can be produced [49]. Figures 3(B)–(C) shows straight channels in a porous scaffold produced by freeze casting the BNC/alginate blend mixture around the inserted clay-needle construct. As seen, the method produces a two-phase hierarchical structure with larger channels surrounded by a porous structure. In a previous study, the porosity of these scaffolds was determined and histogram if the pore size distribution shows that the size of the pores follow a normal distribution where the mean pore size were measured to be 50 ± 25 μm, making it sufficient for cell penetration [54]. It has also been seen that by changing the freezing process the pore size can be changed, making the porosity easily tunable [49].

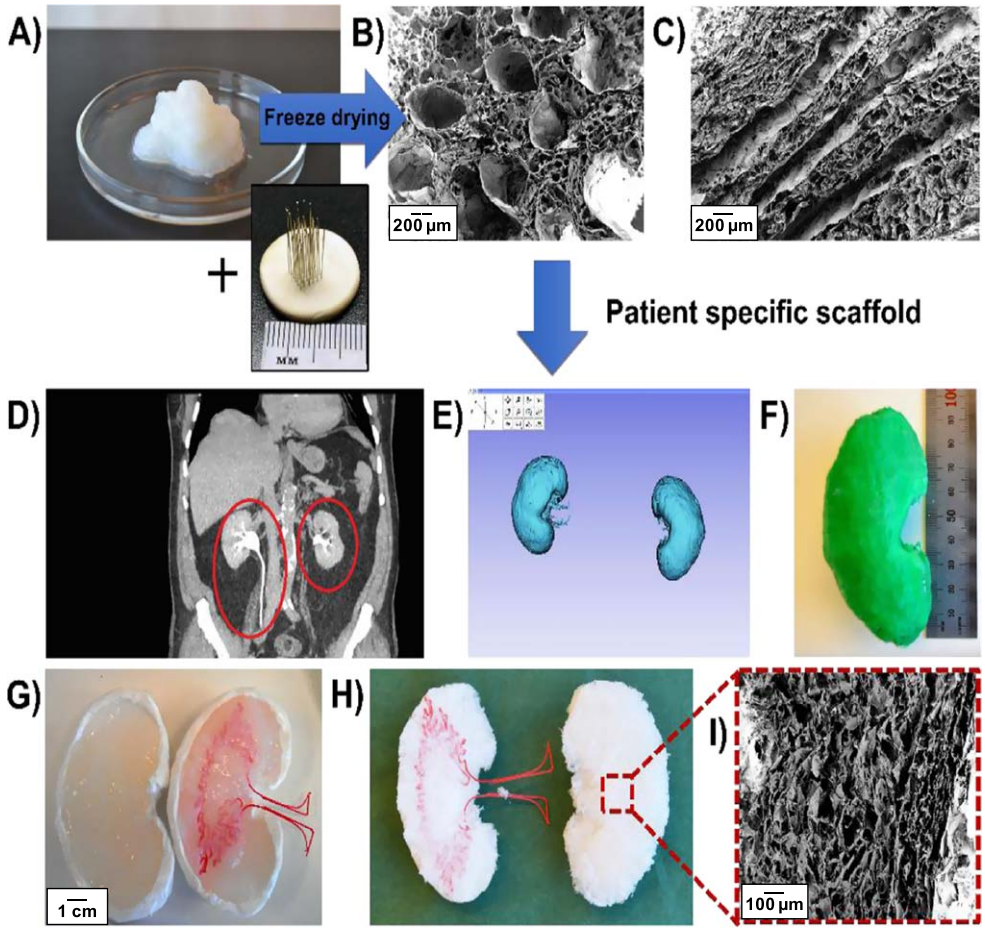

Figure 3. (A) Homogenized BNC blended with alginate (90/10% (w/w)). (B) SEM image of homogenized BNC freeze casted around clay-needle construct perpendicular cut to the channels, (C) cross-sectional cut of the channels. (D) Abdominal computed tomography (CT)-image with kidneys marked in red. The data has been anonymized. (E) .STL-file of kidneys displayed in software Slicer, (F) printed PLA-kidney template, (G) clay-negative filled with homogenized BNC/alginate with an inserted PLA sacrificial template vascular tree, (H) freeze dried BNC/alginate sponge cut in half holding a PLA sacrificial template vascular tree prior to the removal of the template by hydrolysis. (I) SEM image of sponge microstructure.

The ability to customize the macroscopic morphology of a scaffold will enable tailoring to specific patient needs. To demonstrate how the developed technology platform could be utilized, a macro-porous kidney-shaped scaffold was produced by using patient specific data to create a 3D model, which subsequently was used to shape a BNC/alginate sponge scaffold. CT scans of a patient's abdomen (figure 3(D)) were exported as DICOM files and successfully converted to .STL files (figure 3(E)). The .STL files were used to 3D print a full-sized kidney PLA template (figure 3(F)). A clay negative was molded around the printed template, dried and subsequently used to produce a macroscopic kidney mimetic scaffold (figures 3(G)–(H)). Figure 3(I) depicts micro porosity of the scaffold after freeze drying. The successful production of the kidney shaped scaffold showed that macro scaled customized scaffolds can be produced, but further analysis and evaluation is needed to see if an introduced vascular system can support a cell culture in a construct of this size. The BNC/alginate sponge scaffold system without introduced vascular structure has been successfully used together with adipocytes for adipose tissue engineering [49], where it was shown that the scaffolds kept intact during the cell culturing and cells were found in the pores throughout the constructed scaffold. We are currently running promising studies to evaluate the sponge scaffold for hepatocytes, chondrocytes [55] and neuronal cells. Scaffolds with tailored vascular systems could potentially be used to engineer larger constructs utilizing different cell types in co-culture.

Conclusions

In summary, we report on the design, biofabrication and evaluation of BNC scaffolds with a complex vascular mimetic lumen structure. The micro and nanomorphology of the scaffolds facilitate endothelialization and will possibly increase the diffusion of oxygen and nutrients through the scaffolds. In the first part of the study we used a simple needle-clay construct to create the channels in the nanocellulose scaffolds by allowing the bacteria to produce a 3D nanocellulose network around the inserted object in

the fermentation broth. During that process, channels were formed that could be easily perfused and that have a robust structure. The scaffolds were evaluated by showing that HUVECs can attach in the channels of these constructs showing a first step towards vascularization. To further develop the design, a more complex vascular network structure was introduced in the nanoporous BNC scaffolds by using a 3D printer. A 3D print of a tree like structure acted as a sacrificial template to produce a complex channeled network within the BNC during the fermentation process. The channels could be lined with endothelial cells to create a vascular mimetic network. Finally, the possibility to produce larger constructs containing channeled structures as well as pores was investigated. As a proof of concept, patient data from a CT scan was used to create a mold for casting a full-sized kidney-like construct.

Instead of using the fermentation process to produce nanocellulose structure we used a dispersion of nanocellulose with added alginate to provide additional stability to make a slurry. By adding the slurry into the kidney-like construct and then freeze-drying, a porous scaffold with a kidney shape was made. Here, we show that utilizing 3D printing technology together with the use of different BNC scaffolds could allow for a wide range of tissue engineering constructs to be created by tailoring both the type of BNC material being used as well as varying the vascular architecture.

Acknowledgments

Research Council of Norway is greatly acknowledged for funding of the project 3D TUNINK. Daniel Hägg is acknowledged for his assistance with the confocal microscopy analysis. Andreas Hultgren, medical engineer at Karolinska University hospital, is acknowledged for providing CT-data.

ORCID iDs

Kajsa Markstedt https://orcid.org/0000-0001-6737-6887

References

[1] Kaully T, Kaufman-Francis K, Lesman A and Levenberg S 2009 Vascularization—the conduit to viable engineered tissues *Tissue Eng.* B **15** 159–69
[2] Landman K A and Cai A Q 2007 Cell proliferation and oxygen diffusion in a vascularising scaffold *Bull. Math. Biol.* **69** 2405–28
[3] Croll T I, Gentz S, Mueller K, Davidson M, O'Connor A J, Stevens G W and Cooper-White J J 2005 Modelling oxygen diffusion and cell growth in a porous, vascularising scaffold for soft tissue engineering applications *Chem. Eng. Sci.* **60** 4924–34
[4] Rouwkema J, Rivron N C and van Blitterswijk C A 2008 Vascularization in tissue engineering *Trends Biotechnol.* **26** 434–41
[5] Shin M, Matsuda K, Ishii O, Terai H, Kaazempur-Mofrad M, Borenstein J, Detmar M and Vacanti J P 2004 Endothelialized networks with a vascular geometry in microfabricated poly (dimethyl siloxane) *Biomed. Microdevices* **6** 269–78
[6] Hutmacher D W 2001 Scaffold design and fabrication technologies for engineering tissues—state of the art and future perspectives *J. Biomater. Sci. Polym. Ed.* **12** 107–24
[7] Yang S, Leong K-F, Du Z and Chua C-K 2001 The design of scaffolds for use in tissue engineering. I. Traditional factors *Tissue Eng.* **7** 679–89
[8] Kolesky D B, Truby R L, Gladman A, Busbee T A, Homan K A and Lewis J A 2014 3D bioprinting of vascularized, heterogeneous cell-laden tissue constructs *Adv. Mater.* **26** 3124–30
[9] Bertassoni L E, Cecconi M, Manoharan V, Nikkhah M, Hjortnaes J, Cristino A L, Barabaschi G, Demarchi D, Dokmeci M R and Yang Y 2014 Hydrogel bioprinted microchannel networks for vascularization of tissue engineering constructs *Lab Chip* **14** 2202–11
[10] Fuchs S, Ghanaati S, Orth C, Barbeck M, Kolbe M, Hofmann A, Eblenkamp M, Gomes M, Reis R L and Kirkpatrick C J 2009 Contribution of outgrowth endothelial cells from human peripheral blood on *in vivo* vascularization of bone tissue engineered constructs based on starch polycaprolactone scaffolds *Biomaterials* **30** 526–34
[11] Murphy W L, Peters M C, Kohn D H and Mooney D J 2000 Sustained release of vascular endothelial growth factor from mineralized poly(lactide-co-glycolide) scaffolds for tissue engineering *Biomaterials* **21** 2521–7
[12] Shen Y H, Shoichet M S and Radisic M 2008 Vascular endothelial growth factor immobilized in collagen scaffold promotes penetration and proliferation of endothelial cells *Acta Biomater.* **4** 477–89
[13] Lovett M, Lee K, Edwards A and Kaplan D L 2009 Vascularization strategies for tissue engineering *Tissue Eng.* B **15** 353–70
[14] Chang H-I and Wang Y 2011 Cell responses to surface and architecture of tissue engineering scaffolds *Regenerative Medicine and Tissue Engineering—Cells and Biomaterials* ed D Eberli (Rijeka: InTech) pp 569–88
[15] Maidhof R, Marsano A, Lee E J and Vunjak-Novakovic G 2010 Perfusion seeding of channeled elastomeric scaffolds with myocytes and endothelial cells for cardiac tissue engineering *Biotechnol. Prog.* **26** 565–72
[16] Shen J Y, Chan-Park M B E, Feng Z Q, Chan V and Feng Z W 2006 UV-embossed microchannel in biocompatible polymeric film: application to control of cell shape and orientation of muscle cells *J. Biomed. Mater. Res.* B **77** 423–30
[17] Shen J Y, Chan-Park M B, He B, Zhu A P, Zhu X, Beuerman R W, Yang E B, Chen W and Chan V 2006 Three-dimensional microchannels in biodegradable polymeric films for control orientation and phenotype of vascular smooth muscle cells *Tissue Eng.* **12** 2229–40
[18] Kennedy J, McCandless S, Rauf A, Williams L, Hillam J and Hitchcock R 2011 Engineered channels enhance cellular density in perfused scaffolds *Acta Biomater.* **7** 3896–904
[19] Martínez H, Brackmann C, Enejder A and Gatenholm P 2012 Mechanical stimulation of fibroblasts in micro-channeled bacterial cellulose scaffolds enhances production of oriented collagen fibers *J. Biomed. Mater. Res.* A **100** 948–57
[20] Kaihara S, Borenstein J, Koka R, Lalan S, Ochoa E R, Ravens M, Pien H, Cunningham B and Vacanti J P 2000 Silicon micromachining to tissue engineer branched vascular channels for liver fabrication *Tissue Eng.* **6** 105–17
[21] Thomson K S, Korte F S, Giachelli C M, Ratner B D, Regnier M and Scatena M 2013 Prevascularized microtemplated fibrin scaffolds for cardiac tissue engineering applications *Tissue Eng.* A **19** 967–77
[22] Hu X, Huang J, Ye Z, Xia L, Li M, Lv B, Shen X and Luo Z 2009 A novel scaffold with longitudinally oriented microchannels promotes peripheral nerve regeneration *Tissue Eng.* A **15** 3297–308
[23] Lynam D, Bednark B, Peterson C, Welker D, Gao M and Sakamoto J S 2011 Precision microchannel scaffolds for central

and peripheral nervous system repair *J. Mater. Sci., Mater. Med.* **22** 2119–30
[24] Xu T, Jin J, Gregory C, Hickman J J and Boland T 2005 Inkjet printing of viable mammalian cells *Biomaterials* **26** 93–9
[25] Yan Y, Wang X, Pan Y, Liu H, Cheng J, Xiong Z, Lin F, Wu R, Zhang R and Lu Q 2005 Fabrication of viable tissue-engineered constructs with 3D cell-assembly technique *Biomaterials* **26** 5864–71
[26] 2010 *Cell and Organ Printing* (Netherlands: Springer) p 260
[27] Koch L, Gruene M, Unger C and Chichkov B 2013 Laser assisted cell printing *Curr. Pharm. Biotechnol.* **14** 91–7
[28] Markstedt K, Mantas A, Tournier I, Martinez Avila H, Hagg D and Gatenholm P 2015 3D bioprinting human chondrocytes with nanocellulose-alginate bioink for cartilage tissue engineering applications *Biomacromolecules* **16** 1489–96
[29] Hinton T J, Jallerat Q, Palchesko R N, Park J H, Grodzicki M S, Shue H-J, Ramadan M H, Hudson A R and Feinberg A W 2015 Three-dimensional printing of complex biological structures by freeform reversible embedding of suspended hydrogels *Sci. Adv.* **1** e1500758
[30] Melchels F P, Domingos M A, Klein T J, Malda J, Bartolo P J and Hutmacher D W 2012 Additive manufacturing of tissues and organs *Prog. Polym. Sci.* **37** 1079–104
[31] Miller J S, Stevens K R, Yang M T, Baker B M, Nguyen D-H T, Cohen D M, Toro E, Chen A A, Galie P A and Yu X 2012 Rapid casting of patterned vascular networks for perfusable engineered three-dimensional tissues *Nat. Mater.* **11** 768–74
[32] Gao Q, He Y, Fu J-Z, Liu A and Ma L 2015 Coaxial nozzle-assisted 3D bioprinting with built-in microchannels for nutrients delivery *Biomaterials* **61** 203–15
[33] Malda J, Visser J, Melchels F P, Jüngst T, Hennink W E, Dhert W J, Groll J and Hutmacher D W 2013 25th anniversary article: engineering hydrogels for biofabrication *Adv. Mater.* **25** 5011–28
[34] Haigler C H, White A R, Brown R M and Cooper K M 1982 Alteration of *in vivo* cellulose ribbon assembly by carboxymethylcellulose and other cellulose derivatives *J. Cell Biol.* **94** 64–9
[35] Zhang K 2013 Illustration of the development of bacterial cellulose bundles/ribbons by Gluconacetobacter xylinus via atomic force microscopy *Appl. Microbiol. Biotechnol.* **97** 4353–9
[36] Zaborowska M, Bodin A, Bäckdahl H, Popp J, Goldstein A and Gatenholm P 2010 Microporous bacterial cellulose as a potential scaffold for bone regeneration *Acta Biomater.* **6** 2540–7
[37] Helenius G, Bäckdahl H, Bodin A, Nannmark U, Gatenholm P and Risberg B 2006 *In vivo* biocompatibility of bacterial cellulose *J. Biomed. Mater. Res.* A **76** 431–8
[38] Feldmann E-M, Sundberg J, Bobbili B, Schwarz S, Gatenholm P and Rotter N 2013 Description of a novel approach to engineer cartilage with porous bacterial nanocellulose for reconstruction of a human auricle *J. Biomater. Appl.* **28** 626–40
[39] Rosen C L, Steinberg G K, DeMonte F, Delashaw J B J, Lewis S B, Shaffrey M E, Aziz K, Hantel J and Marciano F F 2011 Results of the prospective, randomized, multicenter clinical trial evaluating a biosynthesized cellulose graft for repair of dural defects *Neurosurgery* **69** 1093–104
[40] Ávila H M, Schwarz S, Feldmann E-M, Mantas A, von Bomhard A, Gatenholm P and Rotter N 2014 Biocompatability evaluation of densified bacterial nanocellulose hydrogel as an implant material for aurical cartilage regeneration *Appl. Microbiol. Biotechnol.* **98** 7423–35
[41] Klemm D, Schumann D, Udhardt U and Marsch S 2001 Bacterial synthesized cellulose—artificial blood vessels for microsurgery *Prog. Polym. Sci.* **26** 1561–603
[42] Bäckdahl H, Helenius G, Bodin A, Nannmark U, Johansson B R, Risberg B and Gatenholm P 2006 Mechanical properties of bacterial cellulose and interactions with smooth muscle cells *Biomaterials* **27** 2141–9
[43] Malm C J, Risberg B, Bodin A, Bäckdahl H, Johansson B R, Gatenholm P and Jeppsson A 2012 Small calibre biosynthetic bacterial cellulose blood vessels: 13-months patency in a sheep model *Scand. Cardiovascular J.* **46** 57–62
[44] Nimeskern L, Martínez Ávila H, Sundberg J, Gatenholm P, Müller R and Stok K S 2013 Mechanical evaluation of bacterial nanocellulose as an implant material for ear cartilage replacement *J. Mech. Behav. Biomed. Mater.* **22** 12–21
[45] Schaffner M, Rühs P A, Coulter F, Kilcher S and Studart A R 2017 3D printing of bacteria into functional complex materials *Sci. Adv.* **3** eaao6804
[46] Laromaine A, Tronser T, Pini I, Parets S, Levkin P A and Roig A 2018 Free-standing three-dimensional hollow bacterial cellulose structures with controlled geometry via patterned superhydrophobic–hydrophilic surfaces *Soft Matter* **14** 3955–62
[47] Bäckdahl H, Esguerra M, Delbro D, Risberg B and Gatenholm P 2008 Engineering microporosity in bacterial cellulose scaffolds *J. Tissue Eng. Regen. Med.* **2** 320–30
[48] Chiaoprakobkij N, Sanchavanakit N, Subbalekha K, Pavasant P and Phisalaphong M 2011 Characterization and biocompatibility of bacterial cellulose/alginate composite sponges with human keratinocytes and gingival fibroblasts *Carbohydrate Polym.* **85** 548–53
[49] Krontiras P, Gatenholm P and Hägg D A 2015 Adipogenic differentiation of stem cells in three-dimensional porous bacterial nanocellulose scaffolds *J. Biomed. Mater. Res.* B **103** 195–203
[50] Ahrem H, Pretzel D, Endres M, Conrad D, Courseau J, Müller H, Jaeger R, Kaps C, Klemm D O and Kinne R W 2014 Laser-structured bacterial nanocellulose hydrogels support ingrowth and differentiation of chondrocytes and show potential as cartilage implants *Acta Biomater.* **10** 1341–53
[51] Bodin A, Bharadwaj S, Wu S, Gatenholm P, Atala A and Zhang Y 2010 Tissue-engineered conduit using urine-derived stem cells seeded bacterial cellulose polymer in urinary reconstruction and diversion *Biomaterials* **31** 8889–901
[52] Matsuoka M, Tsuchida T, Matsushita K, Adachi O and Yoshinaga F 1996 A synthetic medium for bacterial cellulose production by Acetobacter xylinum subsp. sucrofermentans *Biosci., Biotechnol., Biochem.* **60** 575–9
[53] MakerBot® Industries, L. http://thingiverse.com (Accessed: 15 February 2013)
[54] Ávila H M, Feldmann E-M, Pleumeekers M M, Nimeskern L, Kuo W, de Jong W C, Schwarz S, Müller R, Hendriks J and Rotter N 2015 Novel bilayer bacterial nanocellulose scaffold supports neocartilage formation *in vitro* and *in vivo* *Biomaterials* **44** 122–33
[55] Feldmann E, Sundberg J F, Bobbili B, Schwarz S, Gatenholm P and Rotter N 2013 Description of a novel approach to engineer cartilage with porous bacterial nanocellulose for reconstruction of a human auricle *J. Biomater. Appl.* **28** 626–40